



Published in final edited form as:

*Anticancer Agents Med Chem.* 2018 ; 18(4): 556–564. doi:10.2174/1871521409666170412115703.

## Synthesis and Evaluation of 2-Naphthaleno *trans*-Stilbenes and Cyanostilbenes as Anticancer Agents

Nikhil R. Madadi<sup>a</sup>, Narsimha R. Penthala<sup>a</sup>, Amit Ketkar<sup>b</sup>, Robert L. Eoff<sup>b</sup>, Vicenta Trujillo-Alonso<sup>c</sup>, Monica L. Guzman<sup>c</sup>, Peter A. Crooks<sup>a,\*</sup>

<sup>a</sup>Department of Pharmaceutical Sciences, College of Pharmacy, University of Arkansas for Medical Sciences, Little Rock, AR 72205, USA;

<sup>b</sup>Department of Biochemistry and Molecular Biology, University of Arkansas for Medical Sciences, Little Rock, AR 72205-7199, USA;

<sup>c</sup>Weill Cornell Medical College, New York, NY 10021, USA

### Abstract

**Background:** Naphthalene is a good structural replacement for the isovanillin moiety (*i.e.* the 3-hydroxy-4-methoxyphenyl unit) in the combretastatin A-4 molecule, a natural product structurally related to resveratrol, which consistently led to the generation of highly cytotoxic naphthalene analogues when combined with a 3,4,5-trimethoxyphenyl or related aromatic system. Also, the naphthalene ring system is present in many current drug molecules that are utilized for anti-tumor, anti-arrhythmia and antioxidant therapy.

**Objective:** In our continuing quest to improve the potencies of naturally occurring anti-cancer molecules through chemical modification, we have now synthesized a small library of 2-naphthaleno *trans*-stilbenes and cyanostilbenes that are structurally related to both resveratrol and DMU-212, and have evaluated these novel analogs against a panel of 54 human tumor cell lines.

**Method:** A series of 2-naphthaleno-containing *trans*-stilbenes **3a-3h** (Scheme 1) were synthesized by Wittig reaction of a variety of aromatic substituted benzyl-triphenylphosphonium bromide reactants with 2-naphthaldehyde using *n*-BuLi as a base in THF. A second series of 2-naphthaleno *trans*-cyanostilbenes analogs **5a-5h** was synthesized by reaction of 2-naphthaldehyde (**2**; 1 mmol) with an appropriately substituted 2-phenylacrylonitrile **4a-4h**; 1 mmol) in 5% sodium methoxide/methanol. The reaction mixture was stirred at room temperature for 2–3 hours and the reaction allowed to go to completion (TLC monitoring), during which time the desired product

\*Address correspondence to this author at the Department of Pharmaceutical, Sciences, College of Pharmacy, University of Arkansas for Medical, Sciences, Little Rock, AR 72205, USA; Tel: +1 5016866495; Fax: +1 5016866057; pacrooks@uams.edu.

#### ETHICS APPROVAL AND CONSENT TO PARTICIPATE

The studies with human cancer cells were carried out by the National Cancer Institute of the USA, and were not done in my laboratory.

#### HUMAN AND ANIMAL RIGHTS

No Animals/Humans were used for studies that are the basis of this research.

#### CONSENT FOR PUBLICATION

Not applicable.

#### CONFLICT OF INTEREST

The authors declare no conflict of interest, financial or otherwise.

precipitated out of the solution as a solid. The resulting precipitate was filtered off, washed with water and dried to yield the desired compound in yields ranging from 70–95% (Scheme 2).

**Results:** The percentage growth inhibition of 54 human cancer cell lines in a primary NCI screen after exposure to compounds **3a**, **3d**, **5b** and **5c** was carried out. The results showed that only compounds **5b** and **5c** met the criteria for subsequent testing to determine growth inhibition values (GI<sub>50</sub>) in dose-response studies. At 10<sup>-5</sup> M concentration, compounds **5b** and **5c** exhibited cytotoxic activity against leukemia cell lines HL-60(TB) and SR, lung cancer cell line NCI-H522, colon cancer cell lines COLO 205 and HCT-116, CNS-cancer cell line SF-539, melanoma cell line MDA-MB-435, and breast cancer cell line BT-549. The naphthalene *trans*-stilbene analogue **3a**, exhibited significant growth inhibition against only one cell line, melanoma cell line MDA-MB-435 (96 % growth inhibition). Compound **3d** was inactive in the 10<sup>-5</sup> M single dose screen.

**Conclusion:** We have synthesized a small set of novel 2-naphthaleno stilbenes and cyanostilbenes and evaluated several of these compounds for their anticancer properties against a panel of 54 human tumor cell lines. The most active analogs, **5b** and **5c**, showed significantly improved growth inhibition against the human cancer cells in the NCI panel when compared to DMU-212. Of these compounds, analog **5c** was found to be the most potent anticancer agent and exhibited significant growth inhibitory effects against COLO 205, CNS SF 539 and melanoma SK-MEL 5 and MDA-MB-435 cell lines with GI<sub>50</sub> values < 25 nM. Analog **5b** also exhibited GI<sub>50</sub> values in the range 25–41 nM against CNS SF 295 and melanoma MDA-MB-435 and UACC-62 cell lines. Compounds **5b** and **5c** were also cytotoxic towards the MV4–11 leukemia cell line with LD<sub>50</sub> value of 450 nM and 200 nM, respectively, and demonstrated >50% inhibition of tubulin polymerization at concentrations below their LD<sub>50</sub> values in these cells. *In silico* docking studies suggest that compounds **5b** and **5c** bind favorably at the colchicine-binding pocket of the tubulin dimer, indicating that both **5b** and **5c** may inhibit tubulin polymerization through a mechanism similar to that exhibited by colchicine. Derivative **5c** demonstrated more favorable binding based on the docking score and buried surface area, as compared to compound **5b**, in agreement with the higher observed potency of **5c** against a broader range of tumor cell lines. Based on these results, analog **5c** is considered to be a lead compound for further optimization as a clinical candidate for treating a variety of cancers.

## Keywords

Resveratrol; DMU-212; naphthalene; growth inhibition; cytotoxicity; tubulin inhibition

## 1. INTRODUCTION

Resveratrol (Fig. 1A) is a phytoalexin which was first isolated and characterized from the medicinal plant *Veratrum album* by Michio Takaoka in 1939 [1]. Since then, this natural product has been isolated from more than 80 other plant species [2]. Resveratrol has received extensive news coverage and is widely used as a supplement drug after being credited with the cardio-protective effects of red wine [3]. In 1991, researchers reported that resveratrol was highly effective in curing skin tumors in mice [4]. Since then, numerous biologically beneficial properties of resveratrol for the treatment of a wide variety of diseases have been reported, including anti-cancer activity, as modulators of platelet aggregation, as an antioxidant [5–7], cardiovascular diseases [8], and in neurodegenerative

diseases [9] in humans. Unfortunately, resveratrol cannot be utilized as a drug product because of its extremely low bioavailability and rapid clearance from the circulation [10].

Extensive anticancer structure-activity relationship (SAR) and metabolic stability studies on resveratrol analogs has revealed that maintaining the stilbene skeleton and replacing the extensively metabolized hydroxyl groups with methoxyl groups improves metabolic stability and retains the medicinal properties of resveratrol [11, 12]. From such SAR studies *trans*-3,4,5,4 tetramethoxystilbene (DMU-212) (Fig. 1B) has been shown to possess more favorable pharmacokinetic properties than resveratrol and exhibits more potent anti-proliferative/proapoptotic activities in a variety of cancer cells, including K562 (leukemia), HT29 (colo-rectal), and HePG2 (hepatoma) HeLa (cervical), LnCaP (prostate), HepG2 (hepatoma) and MCF-7 (breast) cancer cells [13, 14]. Recently, we have reported a comprehensive evaluation of DMU-212 as an anticancer agent against a panel of 54 human tumor cell lines. DMU-212 was found to be an effective antitumor agent against SNB-75 (CNS), MDA-MB-435 (melanoma), A498 (renal) and MCF7 (breast cancer) cell lines, with GI<sub>50</sub> values ranging from 0.74 to 1.88 μM [15].

More recently, we have reported a series of (*Z*)-benzothiophene acrylonitrile derivatives of resveratrol (Fig. 1C); these compounds are potent anti-cancer agents which do not act as substrates for P-glycoproteins [16] involved in cellular efflux mechanisms. Interestingly, Maya *et al.* reported naphthalene to be a good structural replacement for the isovanillin moiety (*i.e.* the 3-hydroxy-4-methoxyphenyl unit) in the combretastatin A-4 molecule, a natural product structurally related to resveratrol, which consistently led to the generation of highly cytotoxic naphthalene analogues (Fig. 1D) when combined with 3,4,5-trimethoxyphenyl or related aromatic systems [17, 18]. Also, the naphthalene ring system is present in many current drug molecules that are utilized for anti-tumor, anti-arrhythmia and antioxidant therapy [19, 20].

In our continuing quest to improve the potencies of naturally occurring anti-cancer molecules through chemical modification, we have now synthesized a small library of 2-naphthaleno *trans*-stilbenes and cyanostilbenes that are structurally related to both resveratrol and DMU-212, and have evaluated these novel analogs against a panel of 54 human tumor cell lines.

## 2. MATERIALS AND METHODS

### 2.1. Chemical Synthesis

All starting materials were purchased from different commercial sources and were used as received without further purification. TLC 60 F254 plates were used for thin layer chromatography (TLC) and silica gel (230–400 mesh) was used for column chromatography. NMR spectra were recorded in CDCl<sub>3</sub>, CDCl<sub>3</sub>+CD<sub>3</sub>OD, or DMSO-d<sub>6</sub> at 400 MHz for <sup>1</sup>H NMR and 100 MHz for <sup>13</sup>C-NMR on an Agilent-400 spectrometer. Chemical shifts (δ) were expressed in parts per million (*ppm*) and coupling constants (*J*) were reported in Hertz (Hz).

## 2.2. Synthesis of Compounds 3a-3h

The series of 2-naphthaleno-containing *trans*-stilbenes **3a-3h** (Scheme 1) were synthesized by Wittig reaction of a series of aromatic substituted benzyl-triphenylphosphonium bromide reactants with 2-naphthaldehyde using *n*-BuLi as a base in THF.

## 2.3. General Procedure for the Synthesis of Compounds 3a-3h

In a round-bottomed flask, an appropriately substituted benzyl-triphenylphosphonium bromide salt (**1a-1h**; 1 mmol) was added to 5 volumes of anhydrous THF under nitrogen gas. The solution was cooled to 0°C in an ice bath and *n*-BuLi (1.2 mmol) was added slowly over a period of 10 min. The reaction was allowed to stir at 0°C for 30 min and 2-naphthaldehyde (**2**; 1 mmol) was added. The reaction was monitored by TLC, and once the reaction was completed, ice water was added to quench the reaction. Ethyl acetate was then added and the organic phase was separated and evaporated under vacuum to afford a crude residue. Silica gel flash chromatography was performed on the crude product to isolate the resulting 2-naphthaleno *trans*-stilbene. Reaction yields obtained for compounds **3a-3h** were within the range 50–70% (Scheme 1).

## 2.4. Analytical Data of Compounds 3a-3h

**(E)-2-(3,5-Dimethoxystyryl)naphthalene (3a)**—<sup>1</sup>H NMR (400 MHz, CDCl<sub>3</sub>): δ 3.85 (s, 6H, OCH<sub>3</sub>), 6.4 (s, 1H, ArH), 6.72 (s, 2H, ArH), 7.18 (m, 2H, Ar-H), 7.46 (m, 2H, ArH), 7.74 (m, 5H, ArH) *ppm*. <sup>13</sup>C NMR (100 MHz, CDCl<sub>3</sub>): δ 55.73 (-OCH<sub>3</sub>), 100.41 (C4), 104.94 (C1 and C6), 123.83, 126.29, 126.69, 127.12, 128.04, 128.35, 128.66, 129.33, 129.62, 133.43, 134.02, 134.97, 139.71, 161.36 (C3 and C5), *ppm*. HRMS calcd. for C<sub>20</sub>H<sub>19</sub>O<sub>2</sub>, (M+H)<sup>+</sup>: 291.1387 Found: 291.1395.

**(E)-2-(4-Ethoxystyryl)naphthalene (3b)**—<sup>1</sup>H NMR (400 MHz, CDCl<sub>3</sub>+CD<sub>3</sub>OD): δ 1.40 (t, *J* = 7.2 Hz, 3H, -CH<sub>3</sub>), 4.03 (dd, *J* = 13.6 Hz, *J* = 6.8 Hz, 2H, -CH<sub>2</sub>), 6.89 (d, *J* = 8.4 Hz, 2H, ArH), 7.10 (d, *J* = 9.2 Hz, 2H, ArH), 7.40–7.49 (m, 4H, ArH), 7.70 (d, 1H, *J* = 8.4 Hz, ArH), 7.79 (m, 4H, ArH) *ppm*. <sup>13</sup>C-NMR (100 MHz, CDCl<sub>3</sub>+CD<sub>3</sub>OD): 14.63 (CH<sub>3</sub>), 63.45 (-OCH<sub>2</sub>), 114.62 (C3 and C5), 123.33, 125.55, 125.95, 126.15, 126.43, 127.53 (-CH=CH-), 127.64, 127.76, 128.10, 128.48, 129.94, 132.73, 133.65, 135.06, 158.57 (C4) *ppm*. HRMS calcd. for C<sub>20</sub>H<sub>19</sub>O, (M+H)<sup>+</sup>: 275.1438 Found: 275.1451.

**(E)-Methyl 4-(2-(naphthalen-2-yl)vinyl)benzoate (3c)**—<sup>1</sup>H NMR (400 MHz, CDCl<sub>3</sub>+CD<sub>3</sub>OD): δ 3.93 (s, 3H, -OCH<sub>3</sub>), 7.28 (s, 1H, ArH), 7.36 (d, *J* = 7.6 Hz, 1H, ArH), 7.47 (m, 2H, ArH), 7.61 (d, *J* = 6.8 Hz, 2H, ArH), 7.74–7.85 (m, 4H, ArH), 7.89 (s, 1H, ArH), 8.03 (d, *J* = 6.8 Hz, 2H, ArH) *ppm*. <sup>13</sup>C NMR (100 MHz, CDCl<sub>3</sub>+CD<sub>3</sub>OD): 52.27 (-OCH<sub>3</sub>), 123.51, 126.41 (-CH=CH-), 126.52, 126.62, 127.50, 127.85, 127.91, 128.24, 128.60, 128.84, 130.20, 131.57, 133.47, 133.77, 134.36, 142.21, 167.49 (-CO) *ppm*. HRMS calcd. for C<sub>20</sub>H<sub>17</sub>O<sub>2</sub>, (M+H)<sup>+</sup>: 289.1230 Found: 289.1252.

**(E)-2-(4-Methoxystyryl)naphthalene (3d)**—<sup>1</sup>H NMR (400 MHz, CDCl<sub>3</sub>): δ 3.82 (s, 3H, -OCH<sub>3</sub>), 6.90 (d, *J* = 8.8 Hz, 2H, ArH), 7.14 (d, *J* = 9.2 Hz, 2H, ArH), 7.41–7.50 (m, 4H, ArH), 7.69 (dd, *J* = 1.2 Hz and 8.4 Hz, 1H, ArH), 7.78–7.80 (m, 4H, ArH) *ppm*. <sup>13</sup>C NMR (100 MHz, CDCl<sub>3</sub>): 55.98 (-OCH<sub>3</sub>), 114.83 (C3 and C5), 124.12, 126.33, 126.77,

126.92, 127.32, 128.33 (-CH=CH-), 128.41, 128.56, 128.89, 129.21, 130.81, 133.50, 134.42, 135.81, 160.01(C4) *ppm*. HRMS calcd. for C<sub>19</sub>H<sub>17</sub>O, (M+H)<sup>+</sup>: 261.1281 Found: 261.1291.

**(E)-2-(3-Methylstyryl)naphthalene (3e)**—<sup>1</sup>H NMR (400 MHz, DMSO-*d*<sub>6</sub>): δ 2.34 (s, 3H, -CH<sub>3</sub>), 7.09–7.26 (d, *J* = 7.2 Hz, 1H, ArH), 7.26 (t, *J* = 7.2 Hz, 1H, ArH), 7.37 (d, *J* = 6.4 Hz, 2H, ArH), 7.43–7.51 (m, 4H, ArH), 7.85–7.92 (m, 4H, ArH), 8.02 (s, 1H, ArH) *ppm*. <sup>13</sup>C NMR (100 MHz, DMSO-*d*<sub>6</sub>): 21.48 (-CH<sub>3</sub>), 124.02, 124.26, 126.41, 126.76, 126.89, 127.49, 128.04, 128.29 (-CH=CH-), 128.64, 128.90, 129.07, 129.47, 132.99, 133.73, 135.15, 137.41, 138.23 (C3) *ppm*. HRMS calcd. for C<sub>19</sub>H<sub>17</sub>, (M+H)<sup>+</sup>: 245.1332 Found: 245.1309.

**(E)-2-(2-Methylstyryl)naphthalene (3f)**—<sup>1</sup>H NMR (400 MHz, DMSO-*d*<sub>6</sub>): δ 2.45 (s, 3H, -CH<sub>3</sub>), 7.19–7.31 (m, 4H, ArH), 7.48–7.59 (m, 3H, ArH), 7.73 (d, *J* = 7.6 Hz, 1H, ArH), 7.89–7.92 (m, 4H, ArH), 8.03 (s, 1H, ArH) *ppm*. <sup>13</sup>C NMR (100 MHz, DMSO-*d*<sub>6</sub>): 20.03 (CH<sub>3</sub>), 124.25, 125.55, 126.43, 126.65, 126.89, 126.92, 128.03 (-CH=CH-), 128.32, 128.63, 130.11, 130.87, 133.03, 133.73, 135.33, 136.07, 136.28 (C1) *ppm*. HRMS calcd. for C<sub>19</sub>H<sub>17</sub>, (M+H)<sup>+</sup>: 245.1332 Found: 245.1322.

**(E)-2-(4-Fluorostyryl)naphthalene (3g)**—<sup>1</sup>H NMR (400 MHz, CDCl<sub>3</sub>): δ 7.04–7.08 (t, *J* = 8.8 Hz, 2H, ArH), 7.17 (s, 2H, ArH), 7.43–7.52 (m, 4H, ArH), 7.69 (dd, *J* = 1.6 Hz, 8.4 Hz, 1H, ArH), 7.80–7.82 (m, 4H, ArH) *ppm*. <sup>13</sup>C NMR (100 MHz, CDCl<sub>3</sub>): 116.22 (C3), 116.43 (C5), 124.05, 126.60, 127.03, 127.24, 128.36 (-CH=CH-), 128.44, 128.63, 128.70, 129.01, 129.20, 129.22, 133.69, 134.18, 134.21, 134.34, 135.30, 161.79, 164.26 (d, C4) *ppm*. HRMS calcd. for C<sub>18</sub>H<sub>14</sub>F, (M+H)<sup>+</sup>: 249.1081 Found: 249.1173.

**(E)-2-(4-Chlorostyryl)naphthalene (3h)**—<sup>1</sup>H NMR (400 MHz, CDCl<sub>3</sub>): δ 7.17 (d, *J* = 14.0 Hz, 2H, ArH), 7.32–7.34 (m, 2H, ArH), 7.44–7.47 (m, 4H, ArH), 7.69 (dd, *J* = 1.6 Hz and 8.4 Hz, 1H, ArH), 7.79–7.83 (m, 4H, ArH) *ppm*. <sup>13</sup>C NMR (100 MHz, CDCl<sub>3</sub>): 123.40, 126.08, 126.44, 126.85, 127.69 (-CH=CH-), 127.70, 127.74, 128.05, 128.41, 128.91, 129.40, 133.14, 133.24, 133.69, 134.49 (C4-Cl), 135.89 (C1) *ppm*. HRMS calcd. for C<sub>18</sub>H<sub>14</sub>Cl, (M+H)<sup>+</sup>: 265.0786 Found: 265.0792.

## 2.5. General Procedure for the Synthesis of Compounds 5a-5h

A second series of 2-naphthaleno *trans*-cyanostilbenes analogs **5a–5h** were synthesized by the reaction of 2-naphthaldehyde (**2**; 1 mmol) with an appropriately substituted 2-phenylacrylonitrile **4a–4h**; 1 mmol) in 5% sodium methoxide/methanol [16].

The reaction mixture was stirred at room temperature for 2–3 hours and the reaction allowed to go to completion (TLC monitoring), during which time the desired product precipitated out of the solution as a solid. The resulting precipitate was filtered off, washed with water and dried to yield the desired compound in yields ranging from 70–95% (Scheme 2).

## 2.6. Analytical Data for Compounds 5a–5h

**(Z)-3-(Naphthalen-2-yl)-2-(4-nitrophenyl)acrylonitrile (5a)**—<sup>1</sup>H NMR (400 MHz, CDCl<sub>3</sub>+CD<sub>3</sub>OD): δ 7.56–7.62 (m, 2H, ArH), 7.86–7.90 (m, 4H, ArH), 7.93 (d, *J* = 9.2 Hz,

2H, ArH), 8.12 (d,  $J = 8.8$  Hz, 1H, ArH), 8.30 (d,  $J = 8.8$  Hz, 2H, ArH), 8.35 (s, 1H, ArH) *ppm*.  $^{13}\text{C}$  NMR (100 MHz,  $\text{CDCl}_3 + \text{CD}_3\text{OD}$ ): 117.67 (=CCN), 124.42 (-CN), 124.64, 125.24, 126.98, 127.38, 128.09, 128.63, 129.24, 129.30, 130.68, 131.95, 133.23, 134.87, 140.99, 145.99 (C4-NO<sub>2</sub>), 148.07 (stilbene =CH) *ppm*. HRMS calcd. for  $\text{C}_{19}\text{H}_{13}\text{N}_2\text{O}_2$ , (M+H)<sup>+</sup>: 301.0979 Found: 301.0756.

**(Z)-2-(3,4-Dimethoxyphenyl)-3-(naphthalen-2-yl)acrylonitrile (5b)**— $^1\text{H}$  NMR (400 MHz,  $\text{CDCl}_3$ ):  $\delta$  3.93 (s, 3H, -OCH<sub>3</sub>), 3.97 (s, 3H, -OCH<sub>3</sub>), 6.91 (d,  $J = 8.0$  Hz, 1H, ArH), 7.19 (d,  $J = 2.4$  Hz, 1H, ArH), 7.29–7.31 (dd,  $J = 2.0$  Hz and 8.4 Hz, 1H, ArH), 7.51–7.54 (m, 2H, ArH), 7.57 (s, 1H, ArH), 7.84–7.91 (m, 3H, ArH), 8.058.07 (dd,  $J = 1.6$  Hz and 8.4 Hz, 1H, ArH), 8.26 (s, 1H, Ar-H) *ppm*.  $^{13}\text{C}$  NMR (100 MHz,  $\text{CDCl}_3$ ): 56.37 (-OCH<sub>3</sub>), 56.39 (-OCH<sub>3</sub>), 109.09 (=C-CN), 111.62 (C6), 111.70 (C1), 118.66 (-CN), 119.41, 125.56, 127.09, 127.78, 127.82, 128.07, 128.99, 129.01, 130.40, 131.74, 133.45, 134.27, 140.70 (stilbene =CH), 149.63 (C3), 150.42 (C4) *ppm*. HRMS calcd. for  $\text{C}_{21}\text{H}_{18}\text{NO}_2$ , (M+H)<sup>+</sup>: 316.1339 Found: 316.1347.

**(Z)-3-(Naphthalen-2-yl)-2-(3,4,5-trimethoxyphenyl)acrylonitrile (5c)**— $^1\text{H}$  NMR (400 MHz,  $\text{CDCl}_3$ ):  $\delta$  3.90 (s, 3H, -OCH<sub>3</sub>), 3.95 (s, 6H, -OCH<sub>3</sub>), 6.91 (s, 2H, ArH), 7.54 (m, 2H, ArH), 7.61 (s, 1H, ArH), 7.84–7.92 (m, 3H, ArH), 8.06 (d,  $J = 1.2$  Hz, 1H, ArH), 8.27 (s, 1H, ArH) *ppm*.  $^{13}\text{C}$  NMR (100 MHz,  $\text{CDCl}_3$ ): 56.65 (OCH<sub>3</sub>), 61.33 (OCH<sub>3</sub>), 104.4 (=C-CN), 111.84, 118.54 (-CN), 125.49, 127.16, 127.97, 128.09, 129.05, 130.59, 130.71, 131.48, 133.41, 134.40, 139.46, 142.03 (stilbene =CH), 153.91 (C3 and C5) *ppm*. HRMS calcd. for  $\text{C}_{22}\text{H}_{20}\text{NO}_3$ , (M+H)<sup>+</sup>: 346.1445 Found: 346.1436.

**(Z)-2-(4-Methoxyphenyl)-3-(naphthalen-2-yl)acrylonitrile (5d)**— $^1\text{H}$  NMR (400 MHz,  $\text{CDCl}_3$ ):  $\delta$  3.84 (s, 3H, -OCH<sub>3</sub>), 6.95 (d,  $J = 8.0$  Hz, 2H, ArH), 7.50–7.53 (m, 2H, ArH), 7.55 (s, 1H, ArH), 7.63 (d,  $J = 8.8$  Hz, 2H, ArH), 7.83–7.89 (m, 3H, ArH), 8.03–8.06 (dd,  $J = 1.2$  Hz and 8.8 Hz, 1H, ArH), 8.24 (s, 1H, ArH) *ppm*.  $^{13}\text{C}$  NMR (100 MHz,  $\text{CDCl}_3$ ): 55.77 (OCH<sub>3</sub>), 111.51 (=C-CN), 114.78 (C3 and C5), 118.66 (-CN), 125.58, 127.06, 127.43, 127.66, 127.76, 128.06, 128.95, 129.01, 130.30, 131.82, 133.45, 134.24, 140.41 (stilbene =CH), 160.77 (C4) *ppm*. HRMS calcd. for  $\text{C}_{20}\text{H}_{16}\text{NO}$ , (M+H)<sup>+</sup>: 286.1234 Found: 286.1258.

**(Z)-3-(Naphthalen-2-yl)-2-phenylacrylonitrile (5e)**— $^1\text{H}$  NMR (400 MHz,  $\text{DMSO}-d_6$ ):  $\delta$  7.47 (t,  $J = 7.2$  Hz, 1H, ArH), 7.54 (t,  $J = 6.8$  Hz, 2H, ArH), 7.60–7.63 (m, 2H, ArH), 7.83 (d,  $J = 7.2$  Hz, 2H, ArH), 7.99 (t,  $J = 13.6$  Hz, 1H, ArH), 8.07 (d,  $J = 8.4$  Hz, 2H, ArH), 8.13 (d,  $J = 8.4$  Hz, 1H, ArH), 8.21 (s, 1H, ArH), 8.43 (s, 1H, ArH) *ppm*.  $^{13}\text{C}$  NMR (100 MHz,  $\text{DMSO}-d_6$ ): 110.91 (=C-CN), 118.51 (-CN), 125.42, 126.23, 126.29, 127.46, 128.16, 128.22, 128.97, 129.69, 129.67, 130.80, 131.81, 133.02, 134.01, 134.30, 143.32, 143.36 (stilbene =CH) *ppm*. HRMS calcd. for  $\text{C}_{19}\text{H}_{14}\text{N}$ , (M+H)<sup>+</sup>: 256.1128 Found: 256.1114.

**(Z)-3-(Naphthalen-2-yl)-2-(3(trifluoromethyl)phenyl)acrylonitrile (5f)**— $^1\text{H}$  NMR (400 MHz,  $\text{CDCl}_3$ ):  $\delta$  7.53–7.60 (m, 3H, ArH), 7.64 (d,  $J = 7.2$  Hz 1H, ArH), 7.71 (s, 1H, ArH), 7.84–7.93 (m, 5H, ArH), 8.08–8.11 (dd,  $J = 2.0$  Hz and 9.2 Hz, 1H, ArH), 8.29 (s, 1H, ArH) *ppm*.  $^{13}\text{C}$  NMR (100 MHz,  $\text{CDCl}_3$ ): 110.69 (=C-CN), 118.34 (-CN), 123.24, 123.28, 125.71 (-CF<sub>3</sub>), 126.38, 126.42, 127.61, 128.45, 128.65, 129.54, 129.99, 130.01, 130.35,

131.34, 131.69, 133.67, 134.99, 136.16, 144.43 (stilbene =CH) *ppm*. HRMS calcd. for C<sub>20</sub>H<sub>13</sub>F<sub>3</sub>N, (M+H)<sup>+</sup>: 324.1002 Found: 324.1026.

**(Z)-2-(Benzo[d][1,3]dioxol-5-yl)-3-(naphthalen-2-yl)acrylonitrile (5g)**—<sup>1</sup>H NMR (400 MHz, CDCl<sub>3</sub>): δ 5.33 (s, 1H, ArH), 5.86 (d, *J* = 12.8 Hz, 2H, OCH<sub>2</sub>O), 6.57 (d, *J* = 8.0 Hz, 1H, ArH), 6.76 (d, *J* = 1.6 Hz, 1H, ArH), 6.84–6.87 (dd, *J* = 1.6 Hz and 8.4 Hz, 1H, ArH), 7.34–7.37 (dd, *J* = 1.6 Hz and 8.8 Hz, 1H, ArH), 7.50–7.52 (m, 2H, ArH), 7.62–7.83 (m, 3H, ArH), 7.88 (s, 1H, =CH) *ppm*. <sup>13</sup>C NMR (100 MHz, CDCl<sub>3</sub>): 101.52 (-OCH<sub>2</sub>O-), 108.41 (=C-CN), 108.44, 121.62 (CN), 121.87, 126.09, 126.61, 126.87, 127.75, 128.19, 128.45, 128.54, 129.33, 130.64, 133.08, 147.87, 148.22 (stilbene =CH) *ppm*. HRMS calcd. for C<sub>20</sub>H<sub>14</sub>NO<sub>2</sub>, (M+H)<sup>+</sup>: 300.1026 Found: 300.1045.

**(Z)-2-(4-Hydroxyphenyl)-3-(naphthalen-2-yl)acrylonitrile (5h)**—<sup>1</sup>H NMR (400 MHz, CDCl<sub>3</sub>+CD<sub>3</sub>OD): δ 6.92–6.95 (dd, *J* = 2.0 Hz and 6.8 Hz, 2H, ArH), 7.53–7.57 (m, 3H, ArH), 7.61–7.63 (dd, *J* = 2.0 Hz and 6.4 Hz, 2H, ArH), 7.89–8.01 (m, 4H, ArH), 8.12 (s, 1H, ArH), 9.94 (s, 1H, -OH) *ppm*. <sup>13</sup>C NMR (100 MHz, CDCl<sub>3</sub>+CD<sub>3</sub>OD): 115.22 (=C-CN), 116.23, 118.25 (-CN), 123.70, 125.71, 125.82, 126.58, 127.04, 127.06, 127.86, 129.10, 130.55, 131.74, 131.78, 133.72, 138.03 (stilbene =CH), 158.54 (C4-OH) *ppm*. HRMS calcd. for C<sub>19</sub>H<sub>14</sub>NO, (M+H)<sup>+</sup>: 272.1077 Found: 272.1084.

### 3. BIOLOGICAL EVALUATION

#### 3.1. Anti-cancer Activity Screening

The National Cancer Institute (NCI) employs an effective triage system for the evaluation of potential anticancer agents based on duplicates already screened and ADME-TOX algorithm results prior to selection of compounds for initial single dose screening assays against a large panel of human cancer cell lines [21]. Of the sixteen 2-naphthaleno *trans*-stilbene and cyanostilbene compounds synthesized, compounds **3a**, **3d**, **5b** and **5c** were selected for anticancer screening against the NCI human cancer cell panel. *In vitro* screening of the above compounds utilized the sulforhodamine B (SRB) assay procedure described by Rubinstein *et al* [21]. Growth inhibitory or cytotoxicity effects of the test molecules were measured by determining percentage cell growth (PG) inhibition after 48 hours incubation. Optical density (OD) measurements of SRB-derived color just before exposing the cells to the test compound (OD<sub>tzero</sub>) and after 48 hours exposure to the test compound (OD<sub>test</sub>) or the control vehicle (OD<sub>ctrl</sub>) were recorded. Compounds were initially screened at 10<sup>-5</sup> M to determine growth inhibition, and only compounds that showed more than 60% growth inhibition in at least eight cell lines from the panel were selected for a complete dose-response study at five different concentrations, *i.e.* 10<sup>-4</sup> M, 10<sup>-5</sup> M, 10<sup>-6</sup> M, 10<sup>-7</sup> M and 10<sup>-8</sup> M, to determine growth inhibition (GI<sub>50</sub>) values.

The percentage growth inhibition of 54 human cancer cell lines in the primary screen after exposure to compounds **3a**, **3d**, **5b** and **5c** are presented in Tables 1S–4S (Supplementary Data). The results showed that only compounds **5b** and **5c** met the criteria for subsequent testing to determine growth inhibition values (GI<sub>50</sub>) in dose-response studies. At 10<sup>-5</sup> M concentration, compounds **5b** and **5c** exhibited cytotoxic activity against leukemia cell lines HL-60(TB) and SR, lung cancer cell line NCI-H522, colon cancer cell lines COLO 205 and

HCT-116, CNS-cancer cell line SF-539, melanoma cell line MDA-MB-435, and breast cancer cell line BT-549. The naphthalene *trans*-stilbene analogue **3a**, exhibited significant growth inhibition against only one cell line, melanoma cell line MDA-MB-435 (96 % growth inhibition). Compound **3d** was inactive in the  $10^{-5}$  M single dose screen.

Table 1 provides data from the five-dose study for compounds **5b**, **5c** and the positive control, **DMU-212**, against the NCI panel of 54 human tumor cell lines. From this study (*Z*)-3-(naphthalen-2-yl)-2-(3,4,5-trimethoxyphenyl)acrylonitrile (**5c**) was identified as the most active compound from the series of 2-naphthaleno *trans*-cyanostilbene analogs, and was found to have significant growth inhibitory effects against a wide variety of human cancer cell lines. Growth inhibition data for **5c** against 4 human cancer cell lines is shown in Fig. (2); GI<sub>50</sub> values were in the range 21–25 nM.

Compound **5c** afforded GI<sub>50</sub> values less than 100 nM against 98% of all the human cancer cell lines in the panel, and exhibited GI<sub>50</sub> values below 50 nM in 73% of the cell lines in the panel. Analog **5c** was significantly effective against the following cancer cell lines: non-small cell lung cancer cell line NCI-H522 (GI<sub>50</sub> = 27 nM), colon cancer cell line COLO 205 (GI<sub>50</sub> = 22 nM), CNS cancer cell lines SF 295 and SF 539 (GI<sub>50</sub> = 28 and 25 nM, respectively), melanoma cell lines M14, MDA-MB-435, and SK-MEL-5 (GI<sub>50</sub> = 26, 21 and 23 nM, respectively), and breast cancer cell lines MDAMB-231/ATCC and MDA-MB-468 (GI<sub>50</sub> = 26 and 27 nM). Compound **5b** showed significant growth inhibitory effects against several human cancer cell lines in the panel, but was generally less potent when compared to lead analog **5c**. Compound **5b** exhibited GI<sub>50</sub> values less than 100 nM against 40% of the human cancer cells in the panel, and afforded GI<sub>50</sub> values less than 50 nM against 14% of the cancer cells in the panel. Analog **5b** specifically afforded significant growth inhibitory effects against colon cancer cell line HCT-116 (GI<sub>50</sub> = 45 nM), CNS cancer cell lines SF 295 and SF 539 (GI<sub>50</sub> = 41 and 49 nM, respectively), melanoma cell lines M14, MDA-MB-435, and UACC-62 (GI<sub>50</sub> = 48, 25, and 35 nM, respectively), and renal cancer cell line A498 (GI<sub>50</sub> = 49 nM). Both **5c** and **5b** showed significantly improved growth inhibitory and cytotoxicity effects against almost all the 54 human tumor cell lines when compared to DMU-212.

### 3.2. Cytotoxicity of **5b** and **5c** Against MV4–11 Cells and Inhibition of Tubulin Polymerization

Compounds **5b** and **5c** were also screened for their *in vitro* cytotoxicity against cultured MV4–11 cells, and for their ability to inhibit tubulin polymerization utilizing both an immunofluorescence assay and antibody against tubulin (a marker for dynamic microtubules) in MV4–11 cells (Fig. 3) [22]. Cultured MV4–11 cells were treated with the above two compounds at seven different doses. Compound **5c** exhibited greater cytotoxicity (LD<sub>50</sub>) towards the MV4–11 leukemia cell line compared to compound **5b** (Fig. 3A). In separate experiments cultured MV4–11 cells were exposed to compounds **5b** and **5c** for 2 hours and cell-based tubulin depolymerization assays performed. Polymerized tubulin in the cell pellet (P) and unpolymerized tubulin in the supernatant (S) were detected by immunoblotting using antibody against tubulin. Compounds **5b** and **5c** both demonstrated

>50% inhibition of tubulin polymerization at concentrations below their LD<sub>50</sub> values, with **5c** being a more potent inhibitor of tubulin polymerization than **5b** (Fig. 3B).

### 3.3. Methodology for Determining the Cytotoxicity of Compounds **5b** and **5c** Against Cultured MV4–11 Cells

MV4–11 cells were cultured in Iscove's Modified Dulbecco's Media (IMDM) supplemented with 100 U/ml penicillin, 100 U/ml streptomycin, and 10% fetal bovine serum (Life technologies). Cells were seeded at  $5 \times 10^5$ /ml, and treated with the test compounds. At 48 hours post treatment, cells were stained with annexin V-FITC (BD Biosciences) and 1  $\mu$ g/ml 7-AAD (Life Technologies). Percent dead cells were determined by flow cytometry as the percent of annexin V+ cells. Data were analyzed using Flowjo 9.3.2 for Mac OS X (TreeStar). Cell death was represented relative to vehicle control (DMSO).

### 3.4. Tubulin Polymerization Inhibition Assay

MV4–11 cells were treated with the indicated doses of compounds **5b** and **5c** for 2 hours. Cells were then lysed in microtubule stabilizing buffer (100 mM PIPES, 1 mM EGTA, 1 mM MgSO<sub>4</sub>, 30% glycerol, 5% DMSO, 1 mM DTT, 0.02% NaN<sub>3</sub>, 0.125% NP-40, pH 6.9) at 37 °C. Free tubulin (supernatants, SN) and polymerized tubulin (pellets, P) were separated and examined by immunoblotting using tubulin antibody. Both microtubule stabilizing and microtubule-destabilizing drugs inhibit hypoxia inducible factor-1 alpha accumulation and activity by disrupting microtubule function [23].

## 4. MOLECULAR DOCKING

In order to determine the molecular mechanism of tubulin inhibition by compounds **5b** and **5c**, we performed *in silico* docking of these molecules to their target, the  $\alpha\beta$ -tubulin dimer. Docking was performed using the web server-based SwissDock [24, 25] as described previously [26]. The tubulin dimer crystal structure PDB 1SA0 was used as the target molecule. The resulting docked poses were ranked based on their Fullfitness (FF) scores, and only the highest-scoring poses for each molecule were considered for further analyses. Manual inspection of the binding modes, determination of atomic interactions, surface area and distance measurements were accomplished using PyMOL (*The PyMOL Molecular Graphics system, v1.8, Schrödinger LLC*).

Similar to our observations earlier with some related resveratrol analogues [26], both compounds **5b** and **5c** docked to the colchicine-binding pocket at the tubulin dimer interface (Fig. 4). As shown in Fig. 4, **5b** and **5c** share most of the atomic interactions with the same set of amino acid residues of tubulin. These interactions consist entirely of van der Waals' contacts and no polar contacts are observed, once again consistent with our observations with related resveratrol analogues. The docking scores of both compounds **5b** and **5c** (Table 2), are in agreement with their observed potencies in the cellular cytotoxicity assay. As indicated in Table 2, compound **5c** shows a higher FF score, as well as a larger buried surface area (859 Å<sup>2</sup>), as compared to **5b** (814 Å<sup>2</sup>).

## CONCLUSION

In conclusion, we have synthesized a small set of novel 2-naphthaleno stilbenes and cyanostilbenes and evaluated several of these compounds for their anticancer properties against a panel of 54 human tumor cell lines. The most active analogs, **5b** and **5c**, showed significantly improved growth inhibition against the human cancer cells in the NCI panel when compared to DMU-212. Of these compounds, analog **5c** was found to be the most potent anticancer agent and exhibited significant growth inhibitory effects against COLO 205, CNS SF 539 and melanoma SK-MEL 5 and MDA-MB-435 cell lines with GI<sub>50</sub> values 25 nM. Analog **5b** also exhibited GI<sub>50</sub> values in the range 25–41 nM against CNS SF 295 and melanoma MDA-MB-435 and UACC-62 cell lines. Compounds **5b** and **5c** were also cytotoxic towards the MV4–11 leukemia cell line with LD<sub>50</sub> value of 450 nM and 200 nM, respectively, and demonstrated >50% inhibition of tubulin polymerization at concentration below their LD<sub>50</sub> values in these cells. *In silico* docking studies suggest that compounds **5b** and **5c** bind favorably at the colchicine-binding pocket of the tubulin dimer, indicating that both **5b** and **5c** may inhibit tubulin polymerization through a mechanism similar to that exhibited by colchicine. Derivative **5c** demonstrated more favorable binding based on the docking score and buried surface area, as compared to compound **5b**, in agreement with the higher observed potency of **5c** against a broader range of tumor cell lines. Based on these results, analog **5c** is considered to be a lead compound for further optimization as a clinical candidate for treating a variety of cancers.

## Supplementary Material

Refer to Web version on PubMed Central for supplementary material.

## ACKNOWLEDGEMENTS

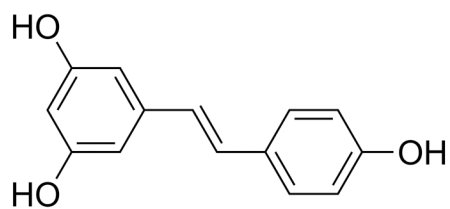
The authors thank the NIH/National Cancer Institute (CA140409), and the Arkansas Research Alliance for financial support. We are also grateful to the NCI Developmental Therapeutic Program (DTP) for anticancer screening data.

## REFERENCES

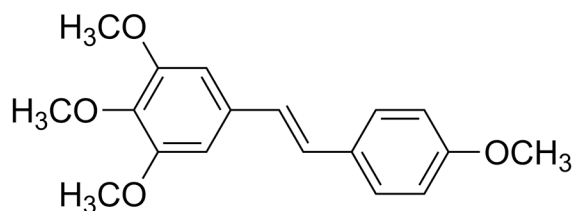
- [1]. Aggarwal BB; Takada Y; Oommen OV From chemoprevention to chemotherapy: common targets and common goals. *Exp. Opin. Investig. Drugs*, 2004, 13(10), 1327–1338.
- [2]. Baur JA; Pearson KJ; Price NL; Jamieson HA; Lerin C; Kalra A; Prabhu VV; Allard JS; Lopez-Lluch G; Lewis K; Pistell PJ; Poosala S; Becker KG; Boss O; Gwinn D; Wang M; Ramaswamy S; Fishbein KW; Spencer RG; Lakatta EG; Le Couteur D; Shaw RJ; Navas P; Puigserver P; Ingram DK; de Cabo R; Sinclair DA Resveratrol improves health and survival of mice on a high-calorie diet. *Nature*, 2006, 444(7117), 337–342. [PubMed: 17086191]
- [3]. Baur JA; Sinclair DA Therapeutic potential of resveratrol: the *in vivo* evidence. *Nat. Rev. Drug. Discov*, 2006, 5(6), 493–506. [PubMed: 16732220]
- [4]. Jang M; Cai L; Udeani GO; Slowing KV; Thomas CF; Beecher CW; Farnsworth NR; Kinghorn AD; Mehta RG; Moon RC; Pezzuto JM Cancer chemopreventive activity of resveratrol, a natural product derived from grapes. *Science*, 1997, 275(5297), 218–220. [PubMed: 8985016]
- [5]. Aggarwal BB; Bhardwaj A; Aggarwal RS; Seeram NP; Shishodia S; Takada Y Role of resveratrol in prevention and therapy of cancer: Preclinical and clinical studies. *Anticancer Res*, 2004, 24(5A), 2783–2840. [PubMed: 15517885]

- [6]. Pace-Asciak CR; Rounova O; Hahn SE; Diamandis EP; Goldberg DM, Wines and grape juices as modulators of platelet aggregation in healthy human subjects. *Clinica. Chimica. Acta*, 1996, 246(1–2), 163–182.
- [7]. Fauconneau B; Waffo-Teguo P; Huguet F; Barrier L; Decendit A; Merillon JM Comparative study of radical scavenger and antioxidant properties of phenolic compounds from *Vitis vinifera* cell cultures using *in vitro* tests. *Life Sci*, 1997, 61(21), 2103–2110. [PubMed: 9395251]
- [8]. Madamanchi NR; Vendrov A; Runge MS Oxidative stress and vascular disease. *Arterioscler. Thromb. Vasc. Biol*, 2005, 25(1), 29–38. [PubMed: 15539615]
- [9]. Vina J; Lloret A; Valles SL; Borrás C; Badia MC; Pallardo FV; Sastre J; Alonso MD Mitochondrial oxidant signalling in Alzheimer’s disease. *J. Alzheimers Dis*, 2007, 11(2), 175–181. [PubMed: 17522442]
- [10]. Greer AK; Madadi NR; Bratton SM; Eddy SD; Mazerska Z; Hendrickson H; Crooks PA; Radominska-Pandya A Novel Resveratrol-Based Substrates for Human Hepatic, Renal and Intestinal UDP-Glucuronosyltransferases. *Chem. Res. Toxicol*, 2014, 27(4), 536–545.
- [11]. Chen Y; Hu F; Gao Y; Jia S; Ji N; Hua E Design, synthesis, and evaluation of methoxylated resveratrol derivatives as potential antitumor agents. *Res. Chem. Intermediat*, 2013, 41(5), 2725–2738.
- [12]. Wang TT; Schoene NW; Kim YS; Mizuno CS; Rimando AM Differential effects of resveratrol and its naturally occurring methylether analogs on cell cycle and apoptosis in human androgen-responsive LNCaP cancer cells. *Mol. Nutr. Food Res*, 2010, 54(3), 335–344. [PubMed: 20077416]
- [13]. Androutsopoulos VP; Ruparelia KC; Papakyriakou A; Filippakis H; Tsatsakis AM; Spandidos DA Anticancer effects of the metabolic products of the resveratrol analogue, DMU-212: Structural requirements for potency. *Euro.J. Med. Chem*, 2011, 46(6), 2586–2595.
- [14]. Sale S; Verschoyle RD; Boocock D; Jones DJL; Wilsher N; Ruparelia KC; Potter GA; Farmer PB; Steward WP; Gescher AJ Pharmacokinetics in mice and growth-inhibitory properties of the putative cancer chemopreventive agent resveratrol and the synthetic analogue *trans* 3,4,5,4[prime]-tetramethoxy stilbene. *Br. J. Cancer*, 2004, 90(3), 736–744. [PubMed: 14760392]
- [15]. Madadi NR; Crooks PA Anticancer evaluation of 3,4,5,4’*trans*-tetramethoxystilbene (DMU-212) and its analogs against an extensive panel of human tumor cell lines. *Lett. Drug Desig. Disco*, 2015, 12(7), 521–528.
- [16]. Penthala NR; Sonar VN; Horn J; Leggas M; Yadlapalli JS; Crooks PA Synthesis and evaluation of a series of benzothiophene acrylonitrile analogs as anticancer agents. *Med.Chem.Comm*, 2013, 4(7), 1073–1078.
- [17]. Maya AB; del Rey B; Lamamie de Clairac RP; Caballero E; Barasoain I; Andreu JM; Medarde M Design, synthesis and cytotoxic activities of naphthyl analogues of combretastatin A-4. *Bioorg. Med. Chem. Lett*, 2000, 10(22), 2549–2551. [PubMed: 11086727]
- [18]. Maya AB; Perez-Melero C; Mateo C; Alonso D; Fernandez JL; Gajate C; Mollinedo F; Pelaez R; Caballero E; Medarde M Further naphthylcombretastatins. An investigation on the role of the naphthalene moiety. *J. Med. Chem*, 2005, 48(2), 556–568. [PubMed: 15658869]
- [19]. Tandon VK; Maurya HK; Mishra NN; Shukla PK Design, synthesis and biological evaluation of novel nitrogen and sulfur containing hetero-1,4-naphthoquinones as potent antifungal and antibacterial agents. *Euro. J. Medi Chem*, 2009, 44(8), 3130–3137.
- [20]. Moussa HH; Abdel Meguid S; El-Hawaary S Novel antimicrobial compounds among naphthalene and methylenedioxy phenyl derivatives. *Pharmazie*, 1981, 36(12), 805–807. [PubMed: 7330082]
- [21]. Rubinstein LV; Shoemaker RH; Paull KD; Simon RM; Tosini S; Skehan P; Scudiero DA; Monks A; Boyd MR Comparison of *in vitro* anticancer-drug-screening data generated with a tetrazolium assay versus a protein assay against a diverse panel of human tumor cell lines. *J. Natl. Cancer Inst*, 1990, 82 (13), 1113–1118. [PubMed: 2359137]
- [22]. Baas PW; Black MM Individual microtubules in the axon consist of domains that differ in both composition and stability. *J. Cell Biol*, 1990, 111(2), 495–509. [PubMed: 2199458]

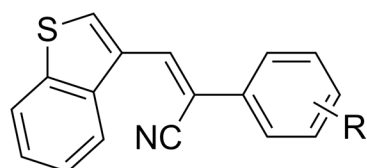
- [23]. Escuin D; Kline ER; Giannakakou P Both microtubule stabilizing and microtubule-destabilizing drugs inhibit hypoxia-inducible factor-1 $\alpha$  accumulation and activity by disrupting microtubule function. *Cancer Res*, 2005, 65(19), 9021–9028. [PubMed: 16204076]
- [24]. Grosdidier A; Zoete V; Michielin O SwissDock, a protein-small molecule docking web service based on EADock DSS. *Nucleic Acids Res*, 2011, 39(Web Server issue), W270–277. [PubMed: 21624888]
- [25]. Grosdidier A; Zoete V; Michielin O Fast docking using the CHARMM force field with EADock DSS. *J. Comput. Chem*, 2011, 32, (10), 2149–2159. [PubMed: 21541955]
- [26]. Madadi NR; Zong H; Ketkar A; Zheng C; Penthala NR; Janganati V; Bommagani S; Eoff RL; Guzman ML; Crooks PA Synthesis and evaluation of a series of resveratrol analogues as potent anti-cancer agents that target tubulin. *Med.Chem. Comm*, 2015, 6(3), 788–794.



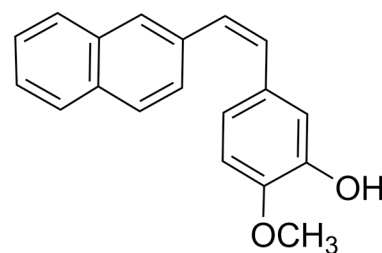
(A) Resveratrol



(B) 3,4,5,4'-trans-tetramethoxystilbene (DMU-212)

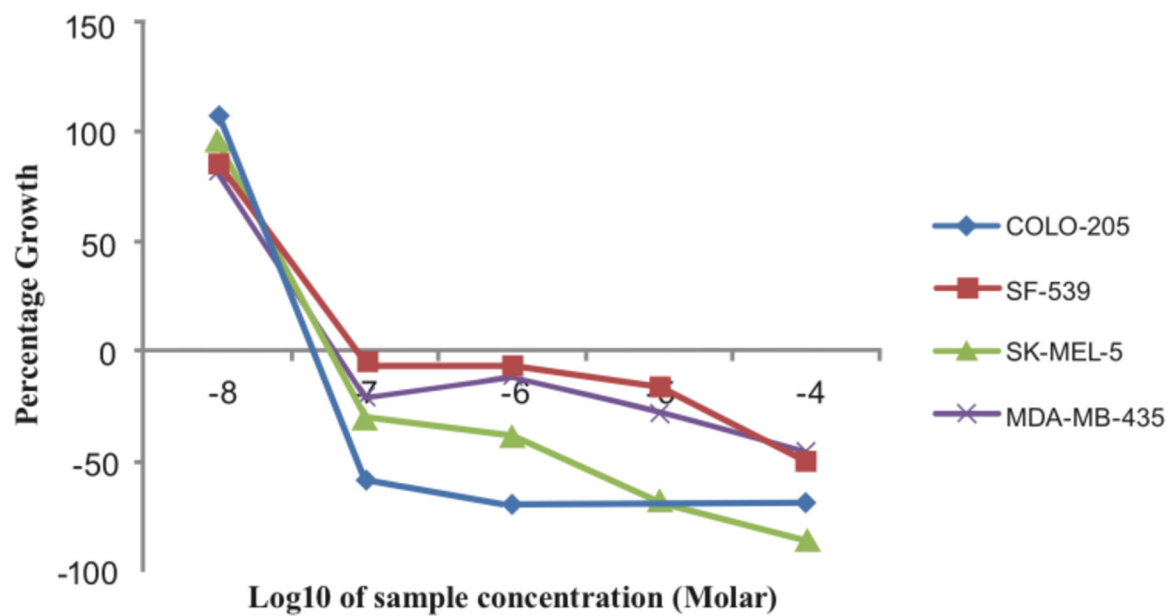


(C) (Z)-Benzothiophene acrylonitriles

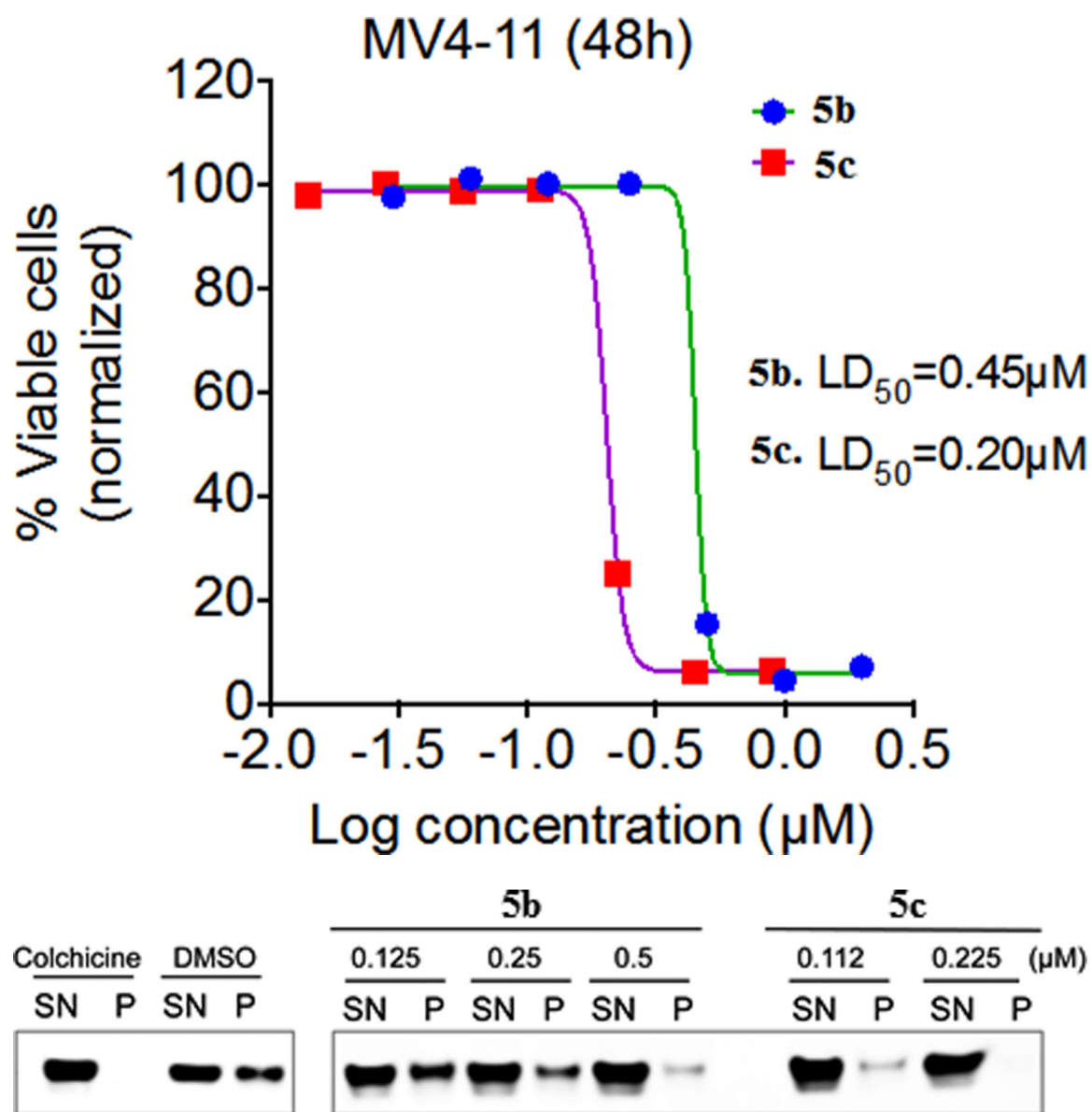


(D) Naphthalene analogues of combretastatin A-4

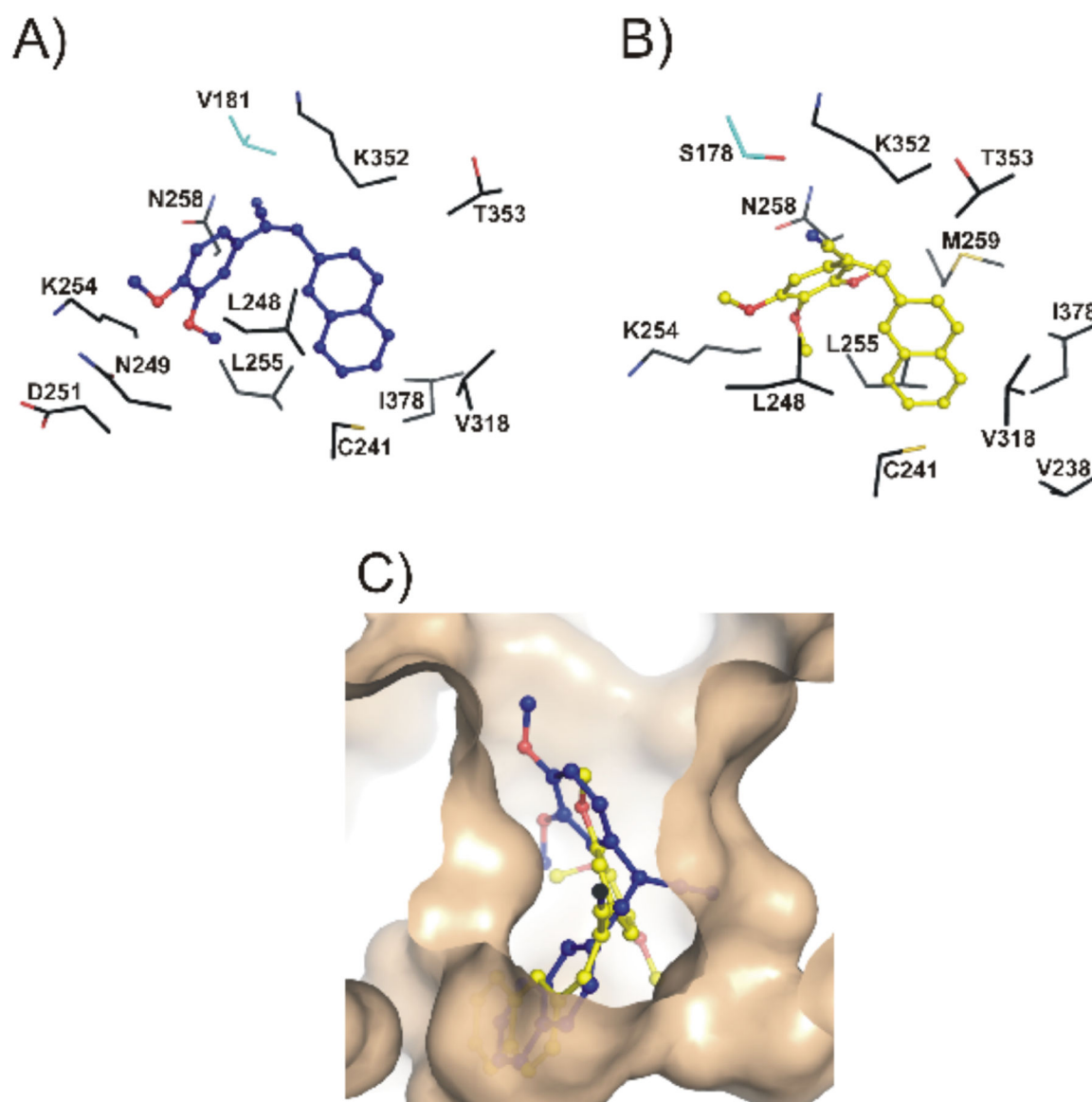
Fig (1). Structures of resveratrol (A), DMU-212 (B), (Z)-benzothiopheneacrylonitriles (C) and the 2-naphthaleno analog of combretastatin A-4 (D).



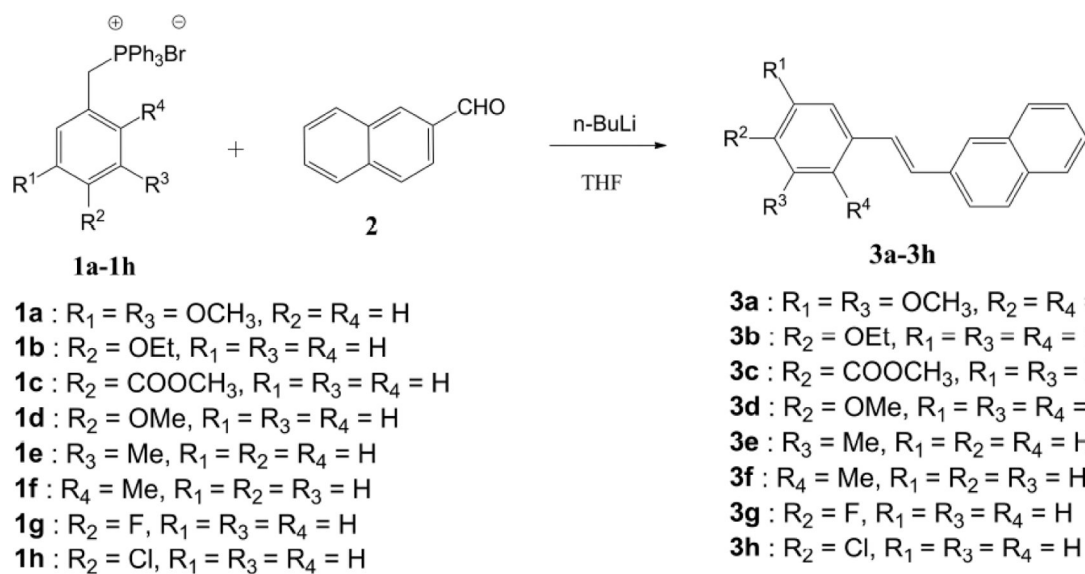
**Fig. (2).**  
Dose-response curves for compound 5c against human colon, CNS, and melanoma cancer cell lines.

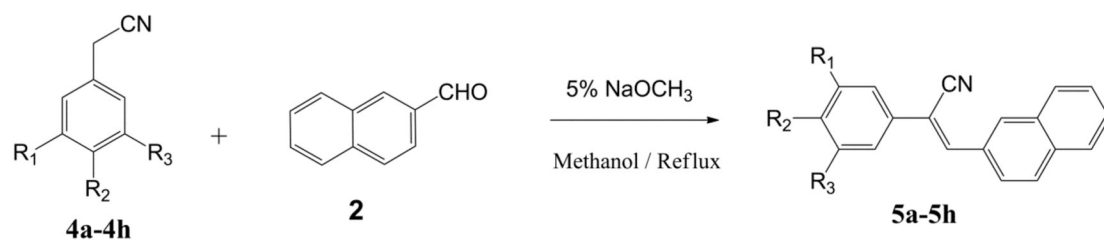


**Fig. (3).**  
Effect of **5b** and **5c** on cell viability (**A**) and tubulin polymerization inhibition (**B**) in MV4-11 leukemia cells.



**Fig. (4).** Compounds **5b**, and **5c** both docked to the colchicine-binding pocket of tubulin. The highest-scoring docked poses of compounds **5b** (blue) and **5c** (yellow) are shown as ball-and-stick models in panels **A** and **B**, respectively. The amino-acid residues of tubulin that are involved in van der Waals' interactions with each molecule are labeled, and are shown as sticks, where  $\alpha$ -tubulin residues are cyan, and the  $\beta$ -tubulin residues are black. Panel **C** shows the top poses of these molecules bound at the colchicine-binding pocket of tubulin, which is shown as a solid surface in wheat. Compound **5b** can be observed to be slightly less deeply buried in the pocket, as compared to **5c**.

**Scheme 1.**Synthesis of 2-naphthaleno *trans*-stilbenes **3a-3h**.



- 4a** : R<sub>2</sub> = NO<sub>2</sub>, R<sub>1</sub> = R<sub>3</sub> = H  
**4b** : R<sub>2</sub> = R<sub>3</sub> = OMe, R<sub>1</sub> = H  
**4c** : R<sub>1</sub> = R<sub>2</sub> = R<sub>3</sub> = OMe  
**4d** : R<sub>2</sub> = OMe, R<sub>1</sub> = R<sub>3</sub> = H  
**4e** : R<sub>1</sub> = R<sub>2</sub> = R<sub>3</sub> = H  
**4f** : R<sub>1</sub> = CF<sub>3</sub>, R<sub>2</sub> = R<sub>3</sub> = H  
**4g** : R<sub>2</sub>R<sub>3</sub> = OMeO, R<sub>1</sub> = H  
**4h** : R<sub>2</sub> = OH, R<sub>1</sub> = R<sub>3</sub> = H

- 5a** : R<sub>2</sub> = NO<sub>2</sub>, R<sub>1</sub> = R<sub>3</sub> = H  
**5b** : R<sub>2</sub> = R<sub>3</sub> = OMe, R<sub>1</sub> = H  
**5c** : R<sub>1</sub> = R<sub>2</sub> = R<sub>3</sub> = OMe  
**5d** : R<sub>2</sub> = OMe, R<sub>1</sub> = R<sub>3</sub> = H  
**5e** : R<sub>1</sub> = R<sub>2</sub> = R<sub>3</sub> = H  
**5f** : R<sub>1</sub> = CF<sub>3</sub>, R<sub>2</sub> = R<sub>3</sub> = H  
**5g** : R<sub>2</sub>R<sub>3</sub> = OMeO, R<sub>1</sub> = H  
**5h** : R<sub>2</sub> = OH, R<sub>1</sub> = R<sub>3</sub> = H

**Scheme 2.**

Synthesis of 2-naphthaleno *trans*-cyanostilbenes **5a-5h**.

Table 1.

Growth inhibition  $GI_{50}^a$  data for compounds **5b**, **5c** and **DMU-212** against a panel of 54 human cancer cell types.

Panel/cell line	<b>5b</b> $GI_{50}^{a,b}$	<b>5c</b> $GI_{50}^{a,b}$	<b>DMU-212</b> $GI_{50}^a$
<b>Leukemia</b>			
CCRF-CEM	0.297	<b>0.052</b>	2.89
HL-60(TB)	<b>0.060</b>	<b>0.031</b>	3.14
MOLT-4	1.010	<b>0.061</b>	3.22
RPMI-8226	0.342	<b>0.053</b>	6.42
SR	<b>0.068</b>	<b>0.032</b>	3.93
<b>Non-Small Cell Lung Cancer</b>			
A549/ATCC	0.146	<b>0.056</b>	3.70
HOP-62	<b>0.095</b>	<b>0.044</b>	3.14
HOP-92	1.410	<b>0.038</b>	7.23
NCI-H226	16.100	NA	4.44
NCI-H23	0.598	<b>0.048</b>	3.37
NCI-H522	<b>0.067</b>	<b>0.027</b>	3.70
<b>Colon Cancer</b>			
COLO 205	0.131	<b>0.022</b>	2.07
HCC-2998	0.331	<b>0.039</b>	3.59
HCT-116	<b>0.045</b>	<b>0.030</b>	3.23
HCT-15	<b>0.057</b>	<b>0.031</b>	2.82
KM12	<b>0.080</b>	<b>0.039</b>	2.32
SW-620	<b>0.054</b>	<b>0.038</b>	3.63
<b>CNS Cancer</b>			
SF-268	0.651	<b>0.051</b>	7.59
SF-295	<b>0.041</b>	<b>0.028</b>	2.18
SF-539	<b>0.048</b>	<b>0.025</b>	2.18
SNB-19	0.414	<b>0.061</b>	4.85
SNB-75	<b>0.091</b>	<b>0.044</b>	1.88
U251	0.218	<b>0.036</b>	3.07
<b>Melanoma</b>			
LOX IMVI	0.145	<b>0.031</b>	4.89
M14	<b>0.048</b>	<b>0.026</b>	2.81
MDA-MB-435	<b>0.025</b>	<b>0.021</b>	1.04
SK-MEL-2	0.558	NA	3.95
SK-MEL-28	0.155	<b>0.049</b>	3.86
SK-MEL-5	<b>0.066</b>	<b>0.023</b>	2.50
UACC-62	<b>0.035</b>	<b>0.039</b>	2.37
<b>Ovarian Cancer</b>			
IGROV1	0.660	<b>0.076</b>	5.29
OVCAR-3	<b>0.051</b>	<b>0.036</b>	3.45
OVCAR-4	0.927	<b>0.077</b>	4.00

Panel/cell line	5b GI <sub>50</sub> <sup>a,b</sup>	5c GI <sub>50</sub> <sup>a,b</sup>	DMU-212 GI <sub>50</sub> <sup>a</sup>
OVCAR-5	0.244	<b>0.033</b>	3.24
OVCAR-8	0.435	<b>0.043</b>	4.54
NCI/ADR-RES	0.244	<b>0.031</b>	3.01
SK-OV-3	0.113	<b>0.030</b>	3.34
<b>Renal Cancer</b> 786-0	<b>0.062</b>	<b>0.035</b>	5.42
A498	<b>0.049</b>	<b>0.033</b>	0.74
ACHN	0.306	<b>0.046</b>	4.51
CAKI-1	<b>0.091</b>	<b>0.051</b>	3.00
RXF 393	<b>0.077</b>	<b>0.054</b>	2.36
SN 12C	0.888	<b>0.056</b>	5.52
TK-10	17.800	<b>0.057</b>	3.98
UO-31	0.761	2.04	3.69
<b>Prostate Cancer</b> PC-3	0.160	<b>0.041</b>	3.22
DU-145	0.381	<b>0.038</b>	4.23
<b>Breast Cancer</b> MCF7	0.157	<b>0.032</b>	1.66
MDA-MB-231/ATCC	0.376	<b>0.026</b>	3.74
HS 578T	0.154	<b>0.038</b>	3.09
BT-549	0.164	<b>0.037</b>	5.13
T-47D	<b>0.064</b>	<b>0.048</b>	3.55
MDA-MB-468	<b>0.094</b>	<b>0.027</b>	2.22

NA: Not analyzed,

<sup>a</sup>GI<sub>50</sub>: 50% Growth inhibition, concentration of drug resulting in a 50% reduction in net protein increase compared with control cells.

<sup>b</sup>GI<sub>50</sub> values <100 nM are bolded.

**Table 2.**

FullFitness (FF) scores and buried surface areas of the highest-scoring pose for **5b** and **5c** molecules docked to tubulin. FF scores were obtained from SwissDock, while the buried surface area was calculated using PyMOL.

Compound	FF score (kcal/mol)	Buried surface area (Å <sup>2</sup> )
<b>5b</b>	4224.9	814
<b>5c</b>	4298.7	859

Author Manuscript

Author Manuscript

Author Manuscript

Author Manuscript